Cluster Assembled Silicon-Lithium Nanostructures: A Nanowire Confined Inside a Carbon Nanotube

Walter Orellana, Ricardo Pino-Rios, Osvaldo Yañez, Alejandro Vásquez-Espinal, Francesca Peccati, Julia Contreras-García, Carlos Cardenas, William Tiznado

frontiers in Chemistry

ORIGINAL RESEARCH
published: 12 November 2021
doi: 10.3389/fchem.2021.767421

Cluster Assembled Silicon-Lithium Nanostructures: A Nanowire Confined Inside a Carbon Nanotube

*Walter Orellana[1], Ricardo Pino-Rios[2], Osvaldo Yañez[3,4], Alejandro Vásquez-Espinal[5], Francesca Peccati[6], Julia Contreras-García[7], Carlos Cardenas[8,9] and William Tiznado[5]**

[1]Departamento de Ciencias Físicas, Universidad Andres Bello, Santiago, Chile, [2]Laboratorio de Química Teórica, Facultad de Química y Biología, Universidad de Santiago de Chile (USACH), Santiago, Chile, [3]Center of New Drugs for Hypertension (CENDHY), Santiago, Chile, [4]Department of Pharmaceutical Science and Technology, School of Chemical and Pharmaceutical Sciences, Universidad de Chile, Santiago, Chile, [5]Departamento de Ciencias Químicas, Computational and Theoretical Chemistry Group, Facultad de Ciencias Exactas, Universidad Andres Bello, Santiago, Chile, [6]Center for Cooperative Research in Biosciences (CIC bioGUNE), Basque Research and Technology Alliance (BRTA), Bizkaia Technology Park, Derio, Spain, [7]Sorbonne Universités, UPMC and CNRS, Laboratoire de Chimie Théorique (LCT), 75005, Paris, France, [8]Departamento de Física, Facultad de Ciencias, Universidad de Chile, Santiago, Chile, [9]Centro para el Desarrollo de la Nanociencias y Nanotecnologia, CEDENNA, Avenida Ecuador, Santiago, Chile

We computationally explore an alternative to stabilize one-dimensional (1D) silicon-lithium nanowires (NWs). The $Li_{12}Si_9$ Zintl phase exhibits the NW $^1_\infty[Li_6Si_5]$, combined with Y-shaped Si_4 structures. Interestingly, this NW could be assembled from the stacking of the Li_6Si_5 aromatic cluster. The $^1_\infty[Li_6Si_5]$@CNT nanocomposite has been investigated with density functional theory (DFT), including molecular dynamics simulations and electronic structure calculations. We found that van der Waals interaction between Li's and CNT's walls is relevant for stabilizing this hybrid nanocomposite. This work suggests that nanostructured confinement (within CNTs) may be an alternative to stabilize this free NW, cleaning its properties regarding $Li_{12}Si_9$ solid phase, i.e., metallic character, concerning the perturbation provided by their environment in the $Li_{12}Si_7$ compound.

Keywords: nanowire, density functional theory, silicon-lithium clusters, carbon nanotube, metallic character

OPEN ACCESS

Edited by:
Iwona Anusiewicz,
University of Gdansk, Poland

Reviewed by:
Fengyu Li,
Inner Mongolia University, China
Tanmoy Chakraborty,
Sharda University, India

****Correspondence:***
William Tiznado
wtiznado@unab.cl

Specialty section:
This article was submitted to Theoretical and Computational Chemistry, a section of the journal Frontiers in Chemistry

Received: *30 August 2021*
Accepted: *01 October 2021*
Published: *12 November 2021*

Citation:
Orellana W, Pino-Rios R, Yañez O, Vásquez-Espinal A, Peccati F, Contreras-García J, Cardenas C and Tiznado W (2021) Cluster Assembled Silicon-Lithium Nanostructures: A Nanowire Confined Inside a Carbon Nanotube. Front. Chem. 9:767421. doi: 10.3389/fchem.2021.767421

INTRODUCTION

The insertion of inorganic materials into single-walled carbon nanotubes (SWCNTs), hereinafter identified simply as CNT, enables the encapsulation of extreme nanowires (NWs) with diameters comparable to a unit cell of the parent material (Green, 1998; Sloan et al., 2002; Spencer et al., 2014). Although NWs of similar diameter can be produced using several templates, such as zeolites (Derouane, 1998), mesoporous phases (Alba-Simionesco et al., 2006; Ke et al., 2009), and metal-organic framework (MOF) (Lu et al., 2012) type materials, CNTs present many advantages as templates; they are atomically smooth, electron transparent, readily available, and can be filled by bulk infiltration to create milligram quantities of encapsulated nanowires, at least on a laboratory scale. Thus, encapsulated NW-CNT are scientifically interesting not only on their own but also as precursors to a wide range of other extreme nanowire materials.

In 2016, Ivanov et al. published a theoretical prediction of helix-shaped lithium-phosphorus nanowires encapsulated into single-walled carbon nanotubes (LiP@CNTs) (Ivanov et al., 2016). Note that helix-shaped Li_nP_n clusters (n = 5–9) had previously been reported as global minimum structures (Ivanov et al., 2012). Some solid phases consist of structural motifs like atomic clusters, i.e., in Zintl phases. This connection brings consistency to the use of models based on

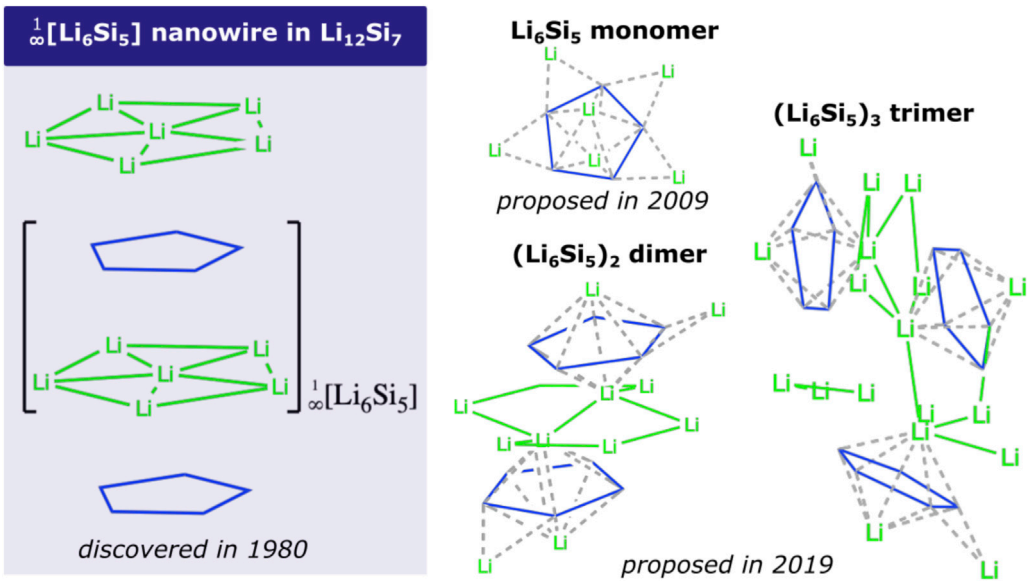

Scheme 1 | Structures of $^{1}_{\infty}[Li_6Si_5]$ NW, Li_6Si_5, $Li_{12}Si_{10}$, and $Li_{18}Si_{15}$ global minima structures, where the square brackets show a repeating unit.

stable clusters to generate NWs inside nanotubes, as proposed in Ivanov's work (Ivanov et al., 2012). The study of these clusters inside CNTs can provide relevant information about these hybrid materials, for example, about their viability (stability analysis), their structural characteristics (geometry analysis), their physical and chemical properties (analysis of their electronic structure).

Due to its excellent energy storage capacity, Si has been extensively studied experimentally as a negative electrode material for Li-ion batteries (Gao et al., 2001; Ryu et al., 2004; Li et al., 2006, Li et al., 2008, Li et al., 2009; Obrovac et al., 2007; Song et al., 2014; Shin et al., 2020). Hence, Si lithifies at high temperature (415°C) in a LiCl-KCl melt, identifying potential plateaus evidencing the crystalline phases $Li_{12}Si_7$, Li_7Si_3, $Li_{13}Si_4$, and $Li_{22}Si_5$ (Wen and Huggins, 1981). In particular, the binary (non-paramagnetic) Zintl-type $Li_{12}Si_7$ silicide contains semi-infinite sandwich-like $^{1}_{\infty}[Li_6Si_5]$ linear chains, consisting of Si_5 pentagons intercalated with Li atoms (see **Scheme 1**). Note that the unit cell of the Zintl $Li_{12}Si_7$ phase has been rationalized (Nesper, 1990; Chevrier et al., 2010; Köster et al., 2011; Kuhn et al., 2011a, Kuhn et al., 2011b) as $(Li_6{}^{6+}[Si_5]_6)_2$ $(Li_{12}{}^{10+}[Si_4]_{10})_2$, with two well-defined silicon moieties: planar Si_5 rings and the Y-shaped Si_4 moiety. Such a structural pattern is justified by assigning 26 electrons (20 from 6Si + 6 from 6Li) to the $Si_5{}^{6-}$ ring, favoring Hückel's aromaticity (Hückel, 1930, Hückel, 1931a, Hückel, 1931b; Zhao et al., 2017). This aromatic character is supported by experimental evidence of an upfield shift (to -17.2 ppm) of Li (at the center of the Li_6 fragment in **Scheme 1**) in the corresponding magic angle NMR (MAS) spectrum (Kuhn et al., 2011b; Köster et al., 2011). It is noteworthy that the $Si_5{}^{6-}$ structural motif is also present in the ternary compound Li_8MgSi_6 (Nesper et al., 1986a). On the other hand, at the cluster level, our group has identified that the global minimum (GM) of the Li_6Si_5 cluster, consists of an aromatic $Si_5{}^{6-}$ pentagon surrounded by 6 Li^+ counterions (Tiznado et al., 2009; Perez-Peralta et al., 2011; Contreras et al., 2013; Vásquez-Espinal et al., 2018). More recently, we have identified the GM structures of the oligomers $(Li_6Si_5)_2$ and $(Li_6Si_5)_3$ (Yañez et al., 2019b; Manrique-de-la-Cuba et al., 2021), which also consist of aromatic Si_5 rings surrounded by Li's (see **Scheme 1**). However, the stacking of Li_6Si_5 units does not tend to form the nanowire identified in $Li_{12}Si_7$, suggesting that $Li_{12}{}^{10+}[Si_4]^{10-}$ component (with the Y-shaped Si_4 moiety) contributes decisively to the stabilization of this NW. In mentioned cluster studies, explorations of the potential energy surface have been performed by hybrid methods, including genetic algorithms (Yañez et al., 2019a, Yañez et al., 2020).

To build new class of materials with desirable properties, using atomic clusters instead of atoms as building blocks, is a remarkable possibility. However, it requires that atomic clusters must retain their identity when assembled, as Khanna and Jena first outlined when they coined the word "cluster-assembled materials" (CAMs) (Khanna and Jena, 1992). These authors argued that the clusters' coupling would have a unique effect on both the assembled material's electronic structure and mechanical properties, which is not possible when the assembly blocks are atoms (Khanna and Jena, 1995; Jena et al., 1996; Jena and Khanna, 1996; Claridge et al., 2009; Jena and Sun, 2018). For a more detailed and timely overview of advances in the assembly of materials from clusters, please refer to the following reviews: (Chakraborty and Pradeep, 2017; Jena and Sun, 2018; Pinkard et al., 2018; Zheng et al., 2019; Doud et al., 2020).

Given the above background, here we evaluated, *in silico*, the stability of the isolated $^{1}_{\infty}[Li_6Si_5]$ NW, as well as its electronic properties. In addition, we studied the hybrid material consisting of the NW confined in a CNT. The latter focused on identifying alternative ways to stabilize this conformation and to evaluate the effect of this association on NW electronic properties. Our density functional theory (DFT) calculations demonstrate that Li-Si@CNTs hybrid systems have excellent stability and thus have potential for experimental realization.

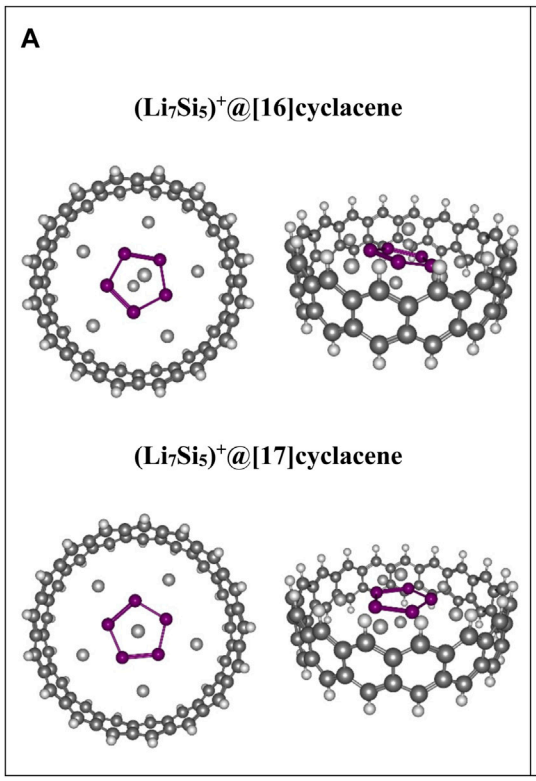

B

$(Li_7Si_5)^+$@[n]cyclacene	E_{int} (kcal mol^{-1})	[n]cyclacene diameter (Å)
n=13	-	10.2
n=14	-	11.0
n=15	-	11.7
n=16	-70.1	12.6
n=17	-62.2	13.3
n=18	-53.0	14.1
n=19	-47.9	14.8
n=20-A	-52.0	15.6
n=20-B	-32.9	

FIGURE 1 | (A) Top-and side-views of optimized structures of $Li_7Si_5^+$ inside both [16]cyclacene and [17]cyclacene at PBE0/def2-TZVP level. **(B)** $Li_7Si_5^+$ and [n] cyclacene interaction energy (E_{int}), number of hexagonal rings and diameter (in Å) of the [n]cyclacene.

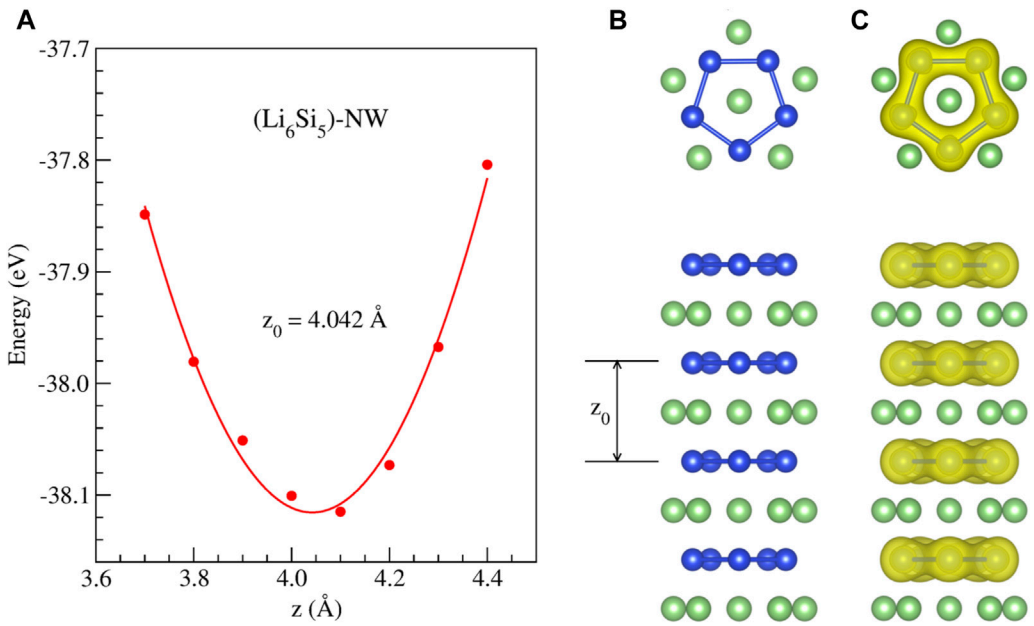

FIGURE 2 | Stability of the $^1_\infty[Li_6Si_5]$ isolated model (Li_6Si_5-NW) obtained from periodic DFT calculations: **(A)** Energy as a function of the distance between Li_6Si_5 units, **(B)** top and side views of the equilibrium geometry, **(C)** electronic density distribution for the isosurface at 0.05 $e/A^{\circ 3}$.

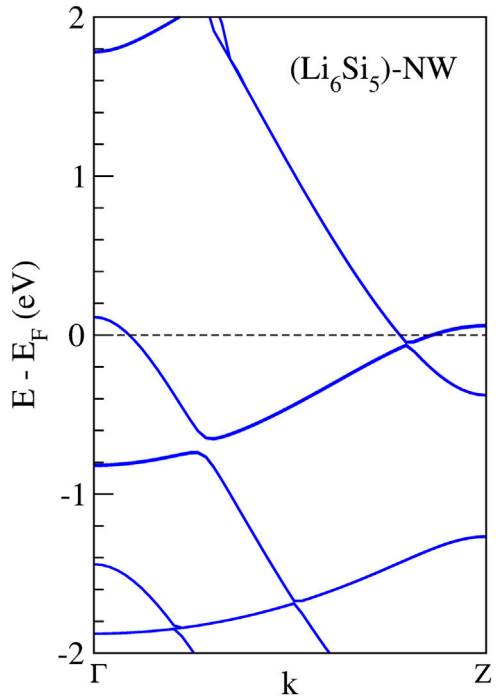

FIGURE 3 | Band structures calculation of the Li_6Si_5-NW in the unit cell. The dashed line indicates the Fermi energy.

COMPUTATIONAL METHODS

In the finite models (clusters), geometry optimizations and frequency calculations were performed at the PBE0 (Adamo and Barone, 1999)/Def2TZVP(Weigend and Ahlrichs, 2005) level with the Gaussian 16 program (M. J. Frisch, G. W. Trucks, H. B. Schlegel et al., 2016).

For the solid-state study, we performed first-principles calculations based on DFT (Sham and Kohn, 1966; Kohn et al., 1996) as implemented in the Vienna Ab Initio Simulation Package (VASP) (Kresse and Furthmüller, 1996). The exchange-correlation energies were calculated at PBE-D3 level (Ernzerhof and Perdew, 1998; Grimme et al., 2010). Plane-wave basis set with a kinetic energy cutoff of 400 eV, and the projector augmented-wave method for the core-valence interaction was employed (Blöchl et al., 1994). The $^{1}_{\infty}[Li_6Si_5]$ NWs were simulated in a large unit cell with volume $(20 \times 20 \times z_0)$ Å^3, considering periodic boundary conditions along the NW direction, where z_0 is the periodicity. Within this supercell, the lateral distance between NW images is set to 15 Å. We use a $(1 \times 1 \times 10)$ Monkhorst-Pack k-point mesh (Monkhorst and Pack, 1976). We also study finite $(Li_6Si_5)_4$ structures in the free space, also inside both an armchair and a zigzag single-walled carbon nanotube (SWCNTs). We consider armchair CNTs with chiral indexes (8,8), (9,9), and (10,10), which have diameters of 10.93, 12.27, and 13.63 Å, and zigzag CNTs with chiral indexes (14,0), (15,0), and (16,0) which have diameters of 11.04, 11.80, and 12.59 Å, respectively. For $(Li_6Si_5)_4$@CNT simulation, $(22 \times 22 \times z_0)$ Å^3 volume was used, where z_0 is the periodicity chosen for the CNTs. All studied structures were allowed to freely relax without any constraint until forces on each atom were smaller than 25 meV/Å. To gain insights on the stability of the NW models in the free space and inside the SWCNTs, we performed Born-Oppenheimer ab initio molecular dynamics (BO-AIMD) simulations within the NVT ensemble at different temperatures, over a total simulation time of 10 ps, considering a time step of 1 fs.

RESULTS AND DISCUSSION

Finite Model Tests to Estimate the Optimal Width of SWNTS

The first question that arises is which is the optimal SWCNT width to favor the $^{1}_{\infty}[Li_6Si_5]$ NW grown? This is a relevant question, considering that the electronic structure of group 1 elements, such as Li, is particularly sensitive to confinement

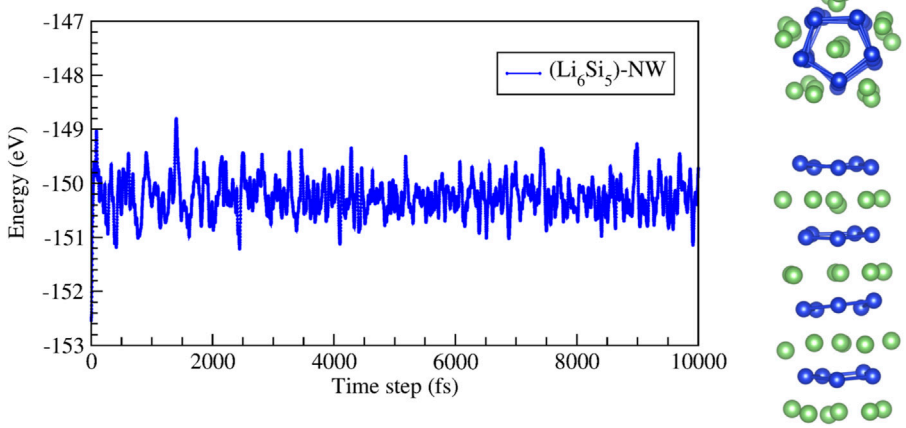

FIGURE 4 | Energy as a function of time for the molecular dynamic simulations at 500 K of the infinite Si_5Li_6 nanowire. The unit cell for this simulation considers four Si_5Li_6 units. The right images show top and side views of a snapshot taken at 10,000 fs

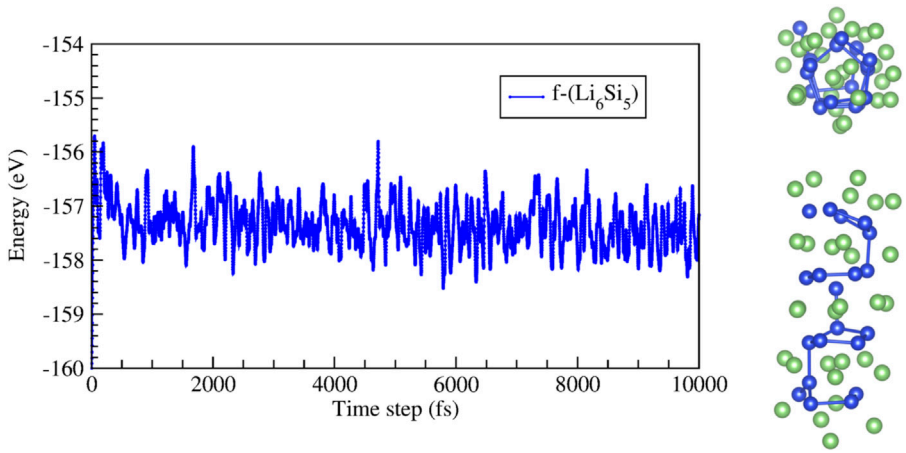

FIGURE 5 | Energy as a function of time for molecular dynamic simulations at 500 K for the finite Li_6Si_5 structure (f-Li_6Si_5). The right images show top and side views of a snapshot taken at 10,000 fs

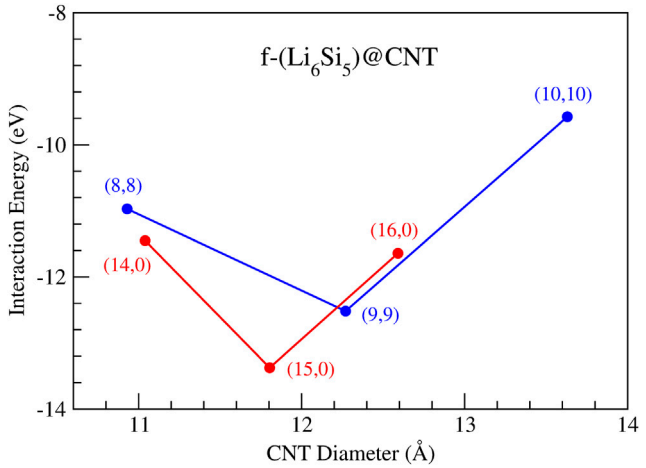

FIGURE 6 | Interaction energy as a function of the nanotube diameters for the finite Li_6Si_5 structures inside armchair CNTs with chiral indexes (8,8), (9,9), and (10,10) and zigzag CNTs with chiral indexes (14,0), (15,0), and (16,0).

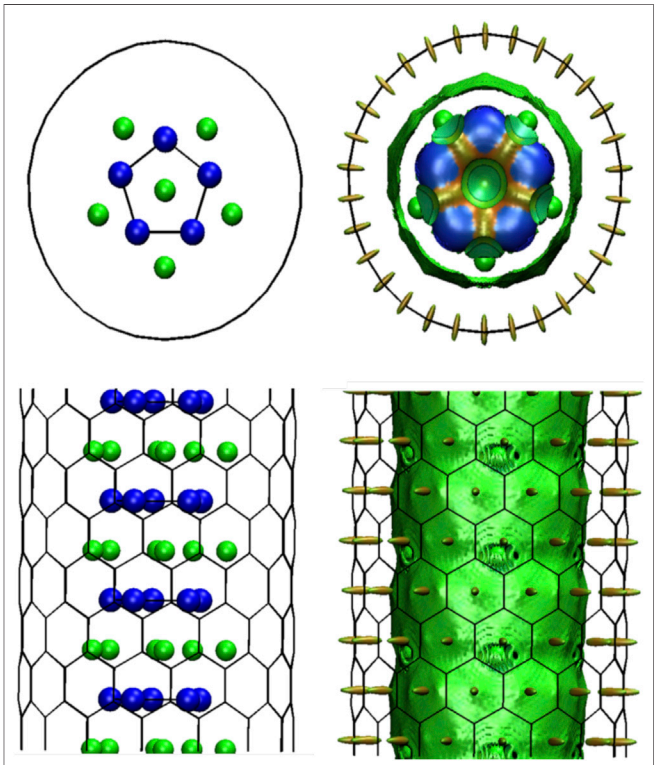

FIGURE 7 | f-Li_6Si_5@NTC optimized structure, for zigzag CNTs with chiral indexes (15,0), with NCI surfaces (s = 0.3, color range: −0.03 to 0.03 a.u.). Geometries and electron density were taken from solid state computations.

(Robles-Navarro et al., 2020). To get an idea of the nanotube widths to be considered in our study, we first performed a finite model analysis. This model consists of [n]cyclacenes (n = 13–20) in their optimal structure (at the PBE0/Def2TZVP level), covering the diameter range from 10.2 to 15.6 Å. Then the $Li_7Si_5^+$ cluster was placed, centering it on emulating the growth pattern towards the nanowire (see **Scheme 1**). We choose the star-shaped D_{5h}-$Li_7Si_5^+$ cluster as a suitable model for projecting the nanowire inside the CNT due to its high symmetry and its analogy in electronic structure with the Li_6Si_5 unit. In this study, we have kept the [n] cyclacene structure rigid, allowing only the optimization of the $Li_7Si_5^+$ structure (at the PBE0/Def2TZVP level).

In the case of small [n]cyclacenes (n = 13–15), $Li_7Si_5^+$ cluster undergoes noticeable changes in the optimization process due to the confinement effects. In contrast, when [n]cyclocenes with n = 16–20 are used, the $Li_7Si_5^+$ cluster maintains its structure at the end of the optimization process, leading to the best interaction energy, [E_{int} = E ($Li_7Si_5^+$at[n]cyclacene)-(E (Li_7Si_5)$^+$E ([n]cyclacene))], with [16] cyclacene (-70.1 kcal mol^{-1} at PBE0/Def2TZVP level). Since this

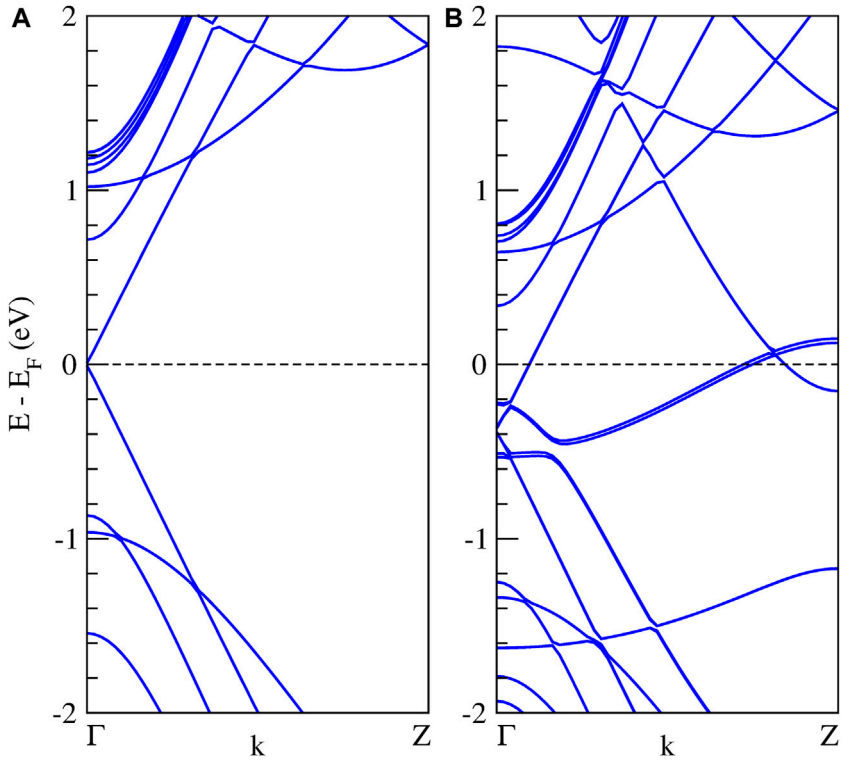

FIGURE 8 | Band structure calculations of the infinite Li_6Si_5-NW inside the zigzag carbon nanotubes, **(A)** the isolated (15,0) CNT, and **(B)** the Li_6Si_5-NW@CNT system. The dashed line indicates the Fermi energy.

analysis is only a reference for estimating the most suitable nanotube diameters to explore in the periodic calculations, we have not included basis set superposition error (BSSE) corrections. The most stable structures, as well as the E_{int}, are shown in **Figure 1**. The structures for the other complexes are shown in **Supplementary Figure S1** and their Cartesian coordinates in **Supplementary Table S1**. These results guided us to use CNTs with diameters in the range of 11–14 Å in next steps of our research.

Insights on the stability of free $^1_\infty[Li_6Si_5]$ NW.

We first studied the stability of periodically repeated Li_6Si_5 units (Li_6Si_5-NW), which are stacked along the *z* direction, forming a one-dimensional structure, as shown in **Figure 2**.

We found a stable structure with an equilibrium distance between Si_5 rings of 4.04 Å which is the periodicity of the Li_6Si_5 unit cell. In the equilibrium geometry, the distance between Li atoms of the border is 3.33 Å while the distance with respect to the center one is 2.83 Å. The Si-Si distance between neighboring atoms is 2.37 Å, very close to the ones in Li_6Si_5 monomer (between 2.30 and 2.35 Å). Our computations of the electronic band structure of the Li_6Si_5-NW in the primitive unit cell suggest a metallic character (see **Figure 3**). Note that the bandgaps of $Li_{12}Si_7$ was reported from conductivity-temperature experimental measurements and found to be 0.6 eV (Nesper et al., 1986b).

The stability of the Li_6Si_5-NW was also verified by BO-AIMD simulations at 300 K and 500K, during a simulation time of 10 ps. The simulation was performed by considering four Li_6Si_5 units in the periodic unit cell, as shown in **Figure 4**. We observe that at 500 K the Si_5Li_6 NW preserves its stability, showing energy fluctuations of around 2 eV. Supporting information contains short movies extracted from the BO-AIMD simulations.

Stability of the Li_6Si_5-NW Inside the CNTs

Next, we studied a finite Li_6Si_5 structure (f-Li_6Si_5) in the free space and encapsulated it inside both armchair and zigzag carbon nanotubes (f-Li_6Si_5@CNT). For the f-Li_6Si_5 structure, we consider four Si_5 rings surrounded by five Li_6 moieties. BO-AIMD simulations provide insights on the stability of the f-Li_6Si_5 system in the free space at 300 K and 500 K. We find that at 300 K, the f-Li_6Si_5 structure preserves its stability. Still, at 500 K, it tends to form Si-Si bonds between adjacent Si rings without losing its one-dimensional array, as shown in **Figure 5**. However, it is important to note that this model does not have the exact stoichiometry of NW because, to maintain symmetry, an extra Li_6 unit group is added, i.e., $[(Li_6)_5(Si_5)_4]$.

To study the f-Li_6Si_5 structure inside the CNTs, we consider three armchair CNTs with chiral indexes of (8,8), (9,9), and (10,10), and three zigzag CNTs with chiral indexes of (14,0), (15,0), and (16,0). With this choice, we seek to find the CNT size that best accommodates the Li_6Si_5-NW inside. Note that we selected these CNTs according to our preliminary findings from the $Li_7Si_5^+$@[n]cyclacene model, suggesting diameters between 12 and 15 Å. The CNTs were simulated with periodic boundary conditions along its axis with a periodicity of z_0 = 30 Å.

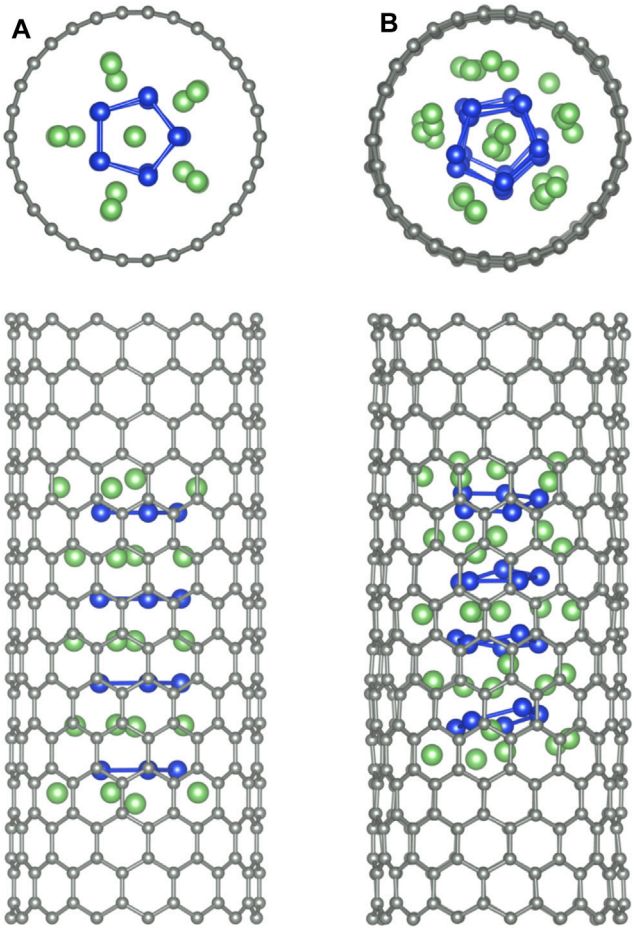

FIGURE 9 | The f-Li_6Si_5 structure inside a zigzag (15,0) CNT. **(A)** Top and side views of the equilibrium geometry at 0 K. **(B)** Top and side views of a snapshot taken at 2000 fs of BO-AIMD simulation at 300 K. The periodicity of the CNT along its axis is z_0 = 30 Å.

The latter allows a vacuum region for the encapsulated f-Li_6Si_5 structure of 14 Å, allowing the atomic movement inside the CNT. Next, we calculate the E_{int} between encapsulated f-Li_6Si_5 and the CNTs by the equation:

$$E_{\text{int}} = E_{tot}\left(f\text{–}Li_6Si_5@CNT\right) - E_{tot}\left(f\text{–}Li_6Si_5\right) - E_{\text{tot}}\left(CNT\right),$$

where $E_{tot}\,(f\text{–}Li_6Si_5)$ and $E_{\text{tot}}\,(\text{CNT})$ are the total energies of the isolated f-Li_6Si_5 and the CNT, respectively, and $E_{\text{tot}}\,(f\text{–}Li_6Si_5@\text{CNT})$ is the total energy of f-Li_6Si_5 unit inside the CNT. Our results for the E_{int} are shown in **Figure 6**. The armchair (9,9) and the zigzag (15,0) CNTs of 12.3 and 11.8 Å in diameter, respectively, exhibit the more stabilizing E_{int}, being the best candidates to accommodate the f-Li_6Si_5 inside. In addition, the f-Li_6Si_5 is better stabilized inside the zigzag (15,0) CNT than inside the armchair (9,9) CNT by 0.9 eV. Noteworthy, the larger-diameter CNTs are energetically less favorable to encapsulate the f-Li_6Si_5, as shown in **Figure 6**, in agreement with the $Li_7Si_5^+$@[n] cyclacene model. This behavior is presumable due to the van der Waals (vdW) interaction between the f-Li_6Si_5 and the CNT internal walls, stabilizing the system. The non-covalent interaction index (NCI) plots confirm the non-covalent character of f-Li_6Si_5 with the CNT [f-Li_6Si_5 inside the zigzag (15,0) CNT]. In the NCI method (Johnson et al., 2010; Contreras-García et al., 2011), an isosurface of the reduced density gradient (s) is colored with the density times the sign of the second eigenvalue of the electron density Hessian matrix, λ_2, to distinguish between attractive and repulsive interactions. The following color code is used: blue for attractive such as hydrogen bonds, green for very weak interactions such as vdW and red for steric repulsion. **Figure 7** depicts the second one (vdW) between f-Li_6Si_5 and the walls of the CNT.

We also calculate the band structure of the Li_6Si_5-NW inside the zigzag (15,0) CNT. It is important to note that the unit cells of the Li_6Si_5-NW and the CNT have a mismatch of 5.7%, which means that the Li_6Si_5-NW is not in its equilibrium geometry in the Li_6Si_5-NW@CNT unit cell, where the distance between the Si_5 rings increases by 0.23 Å. However, this mismatch is relatively small and should not affect the electronic properties of the system. For the isolated CNT we find a small bandgap of 0.02 eV as shown in **Figure 8A**, which is in good agreement with the measured value of 0.029 ± 0.004 eV (Ouyang et al., 2001). Whereas the Li_6Si_5-NW@CNT system exhibits metallic properties as shown **Figure 8B**, suggesting that the Li_6Si_5-NW would preserve its electronic properties inside the CNT as can be compared with **Figure 3**.

Finally, we study the stability of the f-Li_6Si_5 structure inside both zigzag (15,0) and armchair (9,9) CNTs by performing BO-AIMD simulations. **Figure 9A** shows the equilibrium geometry of the f-Si_5Li_6 structure inside the (15,0) CNT. We find that the structure remains almost unchanged with respect to f-Si_5Li_6 in the free space, showing that the CNT would have a small influence in the Li_6Si_5 NW stability. We only note a small displacement of the Li ions at the extreme of the f-Li_6Si_5 structure which move toward the CNT wall. The integrity of the f-Li_6Si_5 structure inside the (15,0) and (9,9) CNTs was investigated by BO-AIMD simulations at 300 K. We find that the f-Si_5Li_6 structure preserves its stability where the Li ions move around the Si_5 ring without detaching. Similar results are found for the f-Li_6Si_5 structure inside the armchair (9,9) CNT, indicating that the formation and stability of the Li_6Si_5 NW inside the CNTs is independent of its chirality. This result suggests that Li_6 Si_5-NW are likely to form inside CNTs in a compact form, which would allow efficient storage of Li ions into CNTs mediated by Si_5 rings. **Supplementary Figure S2** shows the variation of the total energy for the BO-AIMD simulation of f-Li_6Si_5 inside the (15,0) and (9,9) CNTs at 300 K. We observe energy fluctuation of around 5 eV in both CNTs, preserving the stability of the f-Li_6Si_5 structure.

CONCLUSION

Using periodic DFT calculations and Born-Oppenheimer *ab initio* molecular dynamic simulations, we have shown that Li_6Si_5 units can be stacked one above the other, forming a one-dimensional structure linked together by Coulomb interactions. This study complements previous findings, where we

demonstrated that Li_6Si_5, $(Li_6Si_5)_2$, and $(Li_6Si_5)_3$ lowest energy structures contain one, two, and three Si_5^{6-} aromatic rings stabilized by Li^+ counterions. Additionally, the $^1_\infty[Li_6Si_5]$ nanowire was identified in the Zintl $Li_{12}Si_7$ compound but coexisting with Y-shaped Si_4 moieties. In this case, we support the stability of the isolated Si-Li-nanowire—additionally, the relaxed structure (at room temperature) exhibits metallic characteristics.

We also found that finite $(Li_6Si_5)_4$ systems are stable inside both armchair and zigzag carbon nanotubes of around 12 Å in diameter, preserving its stability at room temperature, supporting the viable formation of Li_6Si_5-NW inside the CNTs. Interestingly, the Li_6Si_5-NW@CNTs hybrid nanocomposite maintains the metallic character. Finally, in the Li_6Si_5-NW, the Li_6Si_5 units are connected by strong electrostatic interactions (Si_5^{6-} aromatic pentagons intercalated with the Li_6^{6+} moiety) in agreement with the Zintl ion concept. In the [Li_6Si_5-NW]@CNTs, NCI predicts that Li_6Si_5-NW interacts with the CNT walls by van der Waals interactions Frisch et al., 2016.

DATA AVAILABILITY STATEMENT

The original contributions presented in the study are included in the article/**Supplementary Material**, further inquiries can be directed to the corresponding author.

AUTHOR CONTRIBUTIONS

All authors listed have made a substantial, direct, and intellectual contribution to the work and approved it for publication.

FUNDING

We thank the financial support of National Agency for Research and Development (ANID) through ECOS170045, FONDECYT projects 1211128 (W.T.), 1181121 (C.C.), and 1170480 (W.O.). FONDECYT Postdoctorado 3180119 (R.P.-R.), ANID/PIA ACT192144 (O.Y.). Powered@NLHPC: This research was partially supported by the supercomputing infrastructure of the NLHPC (ECM-02) of the Universidad de Chile. Computational resources for periodic DFT calculations and BO-AIMD simulations were provided by Fenix HCP of the Universidad Andres Bello. C.C. acknowledges Center for the Development of Nanoscience and Nanotechnology CEDENNA AFB180001.

SUPPLEMENTARY MATERIAL

The Supplementary Material for this article can be found online at: https://www.frontiersin.org/articles/10.3389/fchem.2021.767421/full#supplementary-material

REFERENCES

Adamo, C., and Barone, V. (1999). Toward Reliable Density Functional Methods without Adjustable Parameters: The PBE0 Model. *J. Chem. Phys.* 110, 6158–6170. doi:10.1063/1.478522

Alba-Simionesco, C., Coasne, B., Dosseh, G., Dudziak, G., Gubbins, K. E., Radhakrishnan, R., et al. (2006). Effects of Confinement on Freezing and Melting. *J. Phys. Condens. Matter* 18, R15–R68. doi:10.1088/0953-8984/18/6/r01

Blöchl, P. E., Jepsen, O., and Andersen, O. K. (1994). Improved Tetrahedron Method for Brillouin-Zone Integrations. *Phys. Rev. B* 49, 16223–16233. doi:10.1103/physrevb.49.16223

Chakraborty, I., and Pradeep, T. (2017). Atomically Precise Clusters of noble Metals: Emerging Link between Atoms and Nanoparticles. *Chem. Rev.* 117, 8208–8271. doi:10.1021/acs.chemrev.6b00769

Chevrier, V. L., Zwanziger, J. W., and Dahn, J. R. (2010). First Principles Study of Li-Si Crystalline Phases: Charge Transfer, Electronic Structure, and Lattice Vibrations. *J. Alloys Compd.* 496, 25–36. doi:10.1016/j.jallcom.2010.01.142

Claridge, S. A., Castleman, A. W., Jr, Khanna, S. N., Murray, C. B., Sen, A., and Weiss, P. S. (2009). Cluster-assembled Materials. *ACS Nano* 3, 244–255. doi:10.1021/nn800820e

Contreras, M., Osorio, E., Ferraro, F., Puga, G., Donald, K. J., Harrison, J. G., et al. (2013). Isomerization Energy Decomposition Analysis for Highly Ionic Systems: Case Study of Starlike E5Li7+Clusters. *Chem. Eur. J.* 19, 2305–2310. doi:10.1002/chem.201203329

Contreras-García, J., Johnson, E. R., Keinan, S., Chaudret, R., Piquemal, J.-P., Beratan, D. N., et al. (2011). NCIPLOT: A Program for Plotting Noncovalent Interaction Regions. *J. Chem. Theor. Comput.* 7, 625–632. doi:10.1021/ct100641a

Derouane, E. G. (1998). Zeolites as Solid solvents1Paper Presented at the International Symposium `Organic Chemistry and Catalysis' on the Occasion of the 65th Birthday of Prof. H. Van Bekkum, Delft, Netherlands, 2-3 October 1997.1. *J. Mol. Catal. A: Chem.* 134, 29–45. doi:10.1016/s1381-1169(98)00021-1

Doud, E. A., Voevodin, A., Hochuli, T. J., Champsaur, A. M., Nuckolls, C., and Roy, X. (2020). Superatoms in Materials Science. *Nat. Rev. Mater.* 5, 371–387. doi:10.1038/s41578-019-0175-3

Ernzerhof, M., and Perdew, J. P. (1998). Generalized Gradient Approximation to the Angle- and System-Averaged Exchange Hole. *J. Chem. Phys.* 109, 3313–3320. doi:10.1063/1.476928

Frisch, M. J., Trucks, G. W., Schlegel, H. B., Scalmani, G., Robb, M. A., Cheeseman, J. R., et al. (2016). *Gaussian 16, Inc.Revis. B.01*. (Wallingford CT: Gaussian).

Gao, B., Sinha, S., Fleming, L., and Zhou, O. (2001). Alloy Formation in Nanostructured Silicon. *Adv. Mater.* 13, 816–819. doi:10.1002/1521-4095(200106)13:11<816:aid-adma816>3.0.co;2-p

Green, M. H. (1998). The Opening and Filling of Single Walled Carbon Nanotubes (SWTs). *Chem. Commun.* (3), 347–348. doi:10.1039/a707632k

Grimme, S., Antony, J., Ehrlich, S., and Krieg, H. (2010). A Consistent and Accurate Ab Initio Parametrization of Density Functional Dispersion Correction (DFT-D) for the 94 Elements H-Pu. *J. Chem. Phys.* 132, 154104. doi:10.1063/1.3382344

Hückel, E. (1931a). Quanstentheoretische Beitrage Zum Benzolproblem. *Z. Physik* 72, 310–337. doi:10.1007/BF01341953

Hückel, E. (1931b). Quantentheoretische Beitrage Zum Benzolproblem. *Z. Physik* 70, 204–286. doi:10.1007/BF01339530

Hückel, E. (1930). Zur Quantentheorie der Doppelbindung. *Z. Physik* 60, 423–456. doi:10.1007/BF01341254

Ivanov, A. S., Kar, T., and Boldyrev, A. I. (2016). Nanoscale Stabilization of Zintl Compounds: 1D Ionic Li-P Double helix Confined inside a Carbon Nanotube. *Nanoscale* 8, 3454–3460. doi:10.1039/c5nr07713c

Ivanov, A. S., Morris, A. J., Bozhenko, K. V., Pickard, C. J., and Boldyrev, A. I. (2012). Inorganic Double-Helix Structures of Unusually Simple Lithium-Phosphorus Species. *Angew. Chem. Int. Ed.* 51, 8330–8333. doi:10.1002/anie.201201843

Jena, P., and Khanna, S. N. (1996). Physics of Cluster Assembled Materials. *Mater. Sci. Eng. A* 217-218, 218–222. doi:10.1016/s0921-5093(96)10361-0

Jena, P. K., Khanna, S. N., and Rao, B. K. (1996). Stability and Electronic Structure of Cluster Assembled Materials. *Msf* 232, 1–26. doi:10.4028/www.scientific.net/msf.232.1

Jena, P., and Sun, Q. (2018). Super Atomic Clusters: Design Rules and Potential for Building Blocks of Materials. *Chem. Rev.* 118, 5755–5870. doi:10.1021/acs.chemrev.7b00524

Johnson, E. R., Keinan, S., Mori-Sánchez, P., Contreras-García, J., Cohen, A. J., and Yang, W. (2010). Revealing Noncovalent Interactions. *J. Am. Chem. Soc.* 132, 6498–6506. doi:10.1021/ja100936w

Ke, J., Su, W., Howdle, S. M., George, M. W., Cook, D., Perdjon-Abel, M., et al. (2009). Electrodeposition of Metals from Supercritical Fluids. *Proc. Natl. Acad. Sci.* 106, 14768–14772. doi:10.1073/pnas.0901986106

Khanna, S. N., and Jena, P. (1992). Assembling Crystals from Clusters. *Phys. Rev. Lett.* 69, 1664–1667. doi:10.1103/physrevlett.69.1664

Khanna, S. N., and Jena, P. (1995). Atomic Clusters: Building Blocks for a Class of Solids. *Phys. Rev. B* 51, 13705–13716. doi:10.1103/physrevb.51.13705

Kohn, W., Becke, A. D., and Parr, R. G. (1996). Density Functional Theory of Electronic Structure. *J. Phys. Chem.* 100, 12974–12980. doi:10.1021/jp960669l

Köster, T. K.-J., Salager, E., Morris, A. J., Key, B., Seznec, V., Morcrette, M., et al. (2011). Resolving the Different Silicon Clusters in Li12Si7 by 29Si and 6,7Li Solid-State NMR Spectroscopy. *Angew. Chem. Int. Ed.* 50, 12591–12594. doi:10.1002/anie.201105998

Kresse, G., and Furthmüller, J. (1996). Efficient Iterative Schemes Forab Initiototal-Energy Calculations Using a Plane-Wave Basis Set. *Phys. Rev. B* 54, 11169–11186. doi:10.1103/physrevb.54.11169

Kuhn, A., Sreeraj, P., Pöttgen, R., Wiemhöfer, H.-D., Wilkening, M., and Heitjans, P. (2011a). Li Ion Diffusion in the Anode Material Li12Si7: Ultrafast quasi-1D Diffusion and Two Distinct Fast 3D Jump Processes Separately Revealed by 7Li NMR Relaxometry. *J. Am. Chem. Soc.* 133, 11018–11021. doi:10.1021/ja2020108

Kuhn, A., Sreeraj, P., Pöttgen, R., Wiemhöfer, H.-D., Wilkening, M., and Heitjans, P. (2011b). Li NMR Spectroscopy on Crystalline Li12Si7: Experimental Evidence for the Aromaticity of the Planar Cyclopentadienyl-Analogous Si56− Rings. *Angew. Chem. Int. Ed.* 50, 12099–12102. doi:10.1002/anie.201105081

Li, J., Christensen, L., Obrovac, M. N., Hewitt, K. C., and Dahn, J. R. (2008). Effect of Heat Treatment on Si Electrodes Using Polyvinylidene Fluoride Binder. *J. Electrochem. Soc.* 155, A234. doi:10.1149/1.2830545

Li, J., Lewis, R. B., and Dahn, J. R. (2006). Sodium Carboxymethyl Cellulose: A Potential Binder for Si Negative Electrodes for Li-Ion Batteries. *Electrochem. Solid State. Lett.* 10, A17. doi:10.1149/1.2398725

Li, J., Smith, A., Sanderson, R. J., Hatchard, T. D., Dunlap, R. A., and Dahn, J. R. (2009). *In Situ* [sup 119]Sn Mössbauer Effect Study of the Reaction of Lithium with Si Using a Sn Probe. *J. Electrochem. Soc.* 156, A283. doi:10.1149/1.3073879

Lu, G., Li, S., Guo, Z., Farha, O. K., Hauser, B. G., Qi, X., et al. (2012). Imparting Functionality to a Metal-Organic Framework Material by Controlled Nanoparticle Encapsulation. *Nat. Chem* 4, 310–316. doi:10.1038/nchem.1272

Manrique-de-la-Cuba, M. F., Leyva-Parra, L., Inostroza, D., Gomez, B., Vásquez-Espinal, A., Garza, J., et al. (2021). Li8Si8, Li10Si9, and Li12Si10: Assemblies of Lithium-Silicon Aromatic Units. *ChemPhysChem* 22 (10), 906–910. doi:10.1002/cphc.202001051

Monkhorst, H. J., and Pack, J. D. (1976). Special Points for Brillouin-Zone Integrations. *Phys. Rev. B* 13, 5188–5192. doi:10.1103/physrevb.13.5188

Nesper, R., Curda, J., and Von Schnering, H. G. (1986a). Li8MgSi6, a Novel Zintl Compound Containing Quasi-Aromatic Si5 Rings. *J. Solid State. Chem.* 62, 199–206. doi:10.1016/0022-4596(86)90232-x

Nesper, R. (1990). Structure and Chemical Bonding in Zintl-Phases Containing Lithium. *Prog. Solid State. Chem.* 20, 1–45. doi:10.1016/0079-6786(90)90006-2

Nesper, R., von Schnering, H. G., and Curda, J. (1986b). Li12Si7, eine Verbindung mit trigonal-planaren Si4-Clustern und isometrischen Si5-Ringen. *Chem. Ber.* 119, 3576–3590. doi:10.1002/cber.19861191207

Obrovac, M. N., Christensen, L., Le, D. B., and Dahn, J. R. (2007). Alloy Design for Lithium-Ion Battery Anodes. *J. Electrochem. Soc.* 154, A849. doi:10.1149/1.2752985

Ouyang, M., Huang, J.-L., Cheung, C. L., and Lieber, C. M. (2001). Energy Gaps in "Metallic" Single-Walled Carbon Nanotubes. *Science* 292, 702–705. doi:10.1126/science.1058853

Perez-Peralta, N., Contreras, M., Tiznado, W., Stewart, J., Donald, K. J., and Merino, G. (2011). Stabilizing Carbon-Lithium Stars. *Phys. Chem. Chem. Phys.* 13, 12975–12980. doi:10.1039/C1CP21061K

Pinkard, A., Champsaur, A. M., and Roy, X. (2018). Molecular Clusters: Nanoscale Building Blocks for Solid-State Materials. *Acc. Chem. Res.* 51, 919–929. doi:10.1021/acs.accounts.8b00016

Robles-Navarro, A., Fuentealba, P., Muñoz, F., and Cardenas, C. (2020). Electronic Structure of First and Second Row Atoms under Harmonic Confinement. *Int. J. Quan. Chem.* 120, e26132.

Ryu, J. H., Kim, J. W., Sung, Y.-E., and Oh, S. M. (2004). Failure Modes of Silicon Powder Negative Electrode in Lithium Secondary Batteries. *Electrochem. Solid-state Lett.* 7, A306. doi:10.1149/1.1792242

Sham, L. J., and Kohn, W. (1966). One-particle Properties of an Inhomogeneous Interacting Electron Gas. *Phys. Rev.* 145, 561–567. doi:10.1103/physrev.145.561

Shin, H.-J., Hwang, J.-Y., Kwon, H. J., Kwak, W.-J., Kim, S.-O., Kim, H.-S., et al. (2020). Sustainable Encapsulation Strategy of Silicon Nanoparticles in Microcarbon Sphere for High-Performance Lithium-Ion Battery Anode. *ACS Sustain. Chem. Eng.* 8, 14150–14158. doi:10.1021/acssuschemeng.0c04828

Sloan, J., Kirkland, A. I., Hutchison, J. L., and Green, M. L. H. (2002). Integral Atomic Layer Architectures of 1D Crystals Inserted into Single Walled Carbon Nanotubes. *Chem. Commun.* 2010, 1319–1332. doi:10.1039/b200537a

Song, T., Hu, L., and Paik, U. (2014). One-dimensional Silicon Nanostructures for Li Ion Batteries. *J. Phys. Chem. Lett.* 5, 720–731. doi:10.1021/jz4027979

Spencer, J. H., Nesbitt, J. M., Trewhitt, H., Kashtiban, R. J., Bell, G., Ivanov, V. G., et al. (2014). Raman Spectroscopy of Optical Transitions and Vibrational Energies of ~1 Nm HgTe Extreme Nanowires within Single Walled Carbon Nanotubes. *ACS Nano* 8, 9044–9052. doi:10.1021/nn5023632

Tiznado, W., Perez-Peralta, N., Islas, R., Toro-Labbe, A., Ugalde, J. M., and Merino, G. (2009). Designing 3-D Molecular Stars. *J. Am. Chem. Soc.* 131, 9426–9431. doi:10.1021/ja903694d

Vásquez-Espinal, A., Palacio-Rodríguez, K., Ravell, E., Orozco-Ic, M., Barroso, J., Pan, S., et al. (2018). E5M7+ (E= C–Pb, M= Li–Cs): A Source of Viable Star-Shaped Clusters. *Chem. Asian J.* 13, 1751–1755. doi:10.1002/asia.201800654

Weigend, F., and Ahlrichs, R. (2005). Balanced Basis Sets of Split Valence, Triple Zeta Valence and Quadruple Zeta Valence Quality for H to Rn: Design and Assessment of Accuracy. *Phys. Chem. Chem. Phys.* 7, 3297–3305. doi:10.1039/b508541a

Wen, C. J., and Huggins, R. A. (1981). Chemical Diffusion in Intermediate Phases in the Lithium-Silicon System. *J. Solid State. Chem.* 37, 271–278. doi:10.1016/0022-4596(81)90487-4

Yañez, O., Báez-Grez, R., Inostroza, D., Rabanal-León, W. A., Pino-Rios, R., Garza, J., et al. (2019a). AUTOMATON: a Program that Combines a Probabilistic Cellular Automata and a Genetic Algorithm for Global Minimum Search of Clusters and Molecules. *J. Chem. Theor. Comput.* 15, 1463–1475. doi:10.1021/acs.jctc.8b00772

Yañez, O., Garcia, V., Garza, J., Orellana, W., Vásquez-Espinal, A., and Tiznado, W. (2019b). (Li 6 Si 5) 2-5 : The Smallest Cluster-Assembled Materials Based on Aromatic Si 5 6− Rings. *Chem. Eur. J.* 25, 2467–2471. doi:10.1002/chem.201805677

Yañez, O., Inostroza, D., Usuga-Acevedo, B., Vásquez-Espinal, A., Pino-Rios, R., Tabilo-Sepulveda, M., et al. (2020). Evaluation of Restricted Probabilistic Cellular Automata on the Exploration of the Potential Energy Surface of Be6B11−. *Theor. Chem. Acc.* 139, 41. doi:10.1007/s00214-020-2548-5

Zhao, L., Grande-Aztatzi, R., Foroutan-Nejad, C., Ugalde, J. M., and Frenking, G. (2017). Aromaticity, the Hückel 4 N+2 Rule and Magnetic Current. *ChemistrySelect* 2, 863–870. doi:10.1002/slct.201602080

Zheng, X.-Y., Xie, J., Kong, X.-J., Long, L.-S., and Zheng, L.-S. (2019). Recent Advances in the Assembly of High-Nuclearity Lanthanide Clusters. *Coord. Chem. Rev.* 378, 222–236. doi:10.1016/j.ccr.2017.10.023

Conflict of Interest: The authors declare that the research was conducted in the absence of any commercial or financial relationships that could be construed as a potential conflict of interest.

Publisher's Note: All claims expressed in this article are solely those of the authors and do not necessarily represent those of their affiliated organizations, or those of the publisher, the editors and the reviewers. Any product that may be evaluated in this article, or claim that may be made by its manufacturer, is not guaranteed or endorsed by the publisher.